Proceedings of the 25th International Conference on
Port and Ocean Engineering under Arctic Conditions
June 9-13, 2019, Delft, The Netherlands

The Effect of Sample Dimensions on the Compressive Strength of Model-scale Ice

Mikko T.O. Suominen[1], Rüdiger U. Franz von Bock und Polach[2], Andrea Haase[1]
[1] Hamburg Ship Model Basin (HSVA), Hamburg, Germany
[2] Hamburg University of Technology (TUHH), Hamburg, Germany

ABSTRACT

Ice going vessels are commonly designed to break the ice cover through bending. However, due to the increasing interest in activities in the Arctic, the number of structures entering the ice covered sea areas with an unconventional ice breaking design and operational profiles increases. Thus, scaling the compressive strength of model-scale ice correctly gains significance.

In order to avoid the effect of measurement methods on the resulting compressive strength, the methods should be comparable between the full and model-scale and between the model testing facilities. Thus, International Towing Tank Conference (ITTC) gives recommendations on the testing procedures. ITTC (2014) gives two different length-width ratios for the compressive strength specimen. However, as stated in the recommendations and noted by earlier studies (Li and Riska, 1996; von Bock und Polach and Ehlers, 2015), the specimen dimensions affect the determined nominal compressive strength.

A series of measurements is conducted ex-situ in the Large Ice Model Basin of The Hamburg Ship Model Basin (HSVA) within EU funded project Hydralab+. This report presents the findings from the tests and compares them to the former works. The results show that the length-width ratio of the compressive strength sample affects the measured compressive strength, failure pattern, and the strain modulus determined from the compressive strength measurements. Additionally, there are indications that different failure developments in-situ and ex-situ occur and it needs to be investigated to what extend those affect the compressive strength.

KEY WORDS: Model-scale ice; Compressive strength; Aspect ratio; Columnar saline ice; Strain modulus; Failure pattern

INTRODUCTION

Background and Scope of Work

The flexural strength and thickness may be considered as key parameters in modelling an ice sheet for conventional icebreaker shaped ships and sloping structures. Other important characteristics, such as the Young's or strain modulus, are modelled indirectly, as those are a function of other adjustments necessary to establish the desired flexural strength. In this regard, the common practice is that the dimensionless ratio of the flexural strength with other strength parameters should be at the same range as in the nature, e.g. the ratio of the elastic modulus to the flexural strength is to be larger than 2000 (Schwarz, 1977). As the ratios are dimensionless, the ratios should be identical in model and full-scale.

The compressive strength is, similar to the strain modulus, a parameter depending on the flexural strength in model-scale. The compressive strength is commonly defined as a peak force divided by the nominal cross-sectional area of the sample. Lau et al. (2007) estimated with coarse calculations that the ratio between the compressive and flexural strength in nature ranges from 1.8 to 5. However, the compressive behavior of ice and its impact on structures is highly manifold. This ranges from strain-rate dependencies (Sinha, 1984) to tri-axial stress states (Jordaan, 2001). The compressive strength depends on a multitude of parameters of which strain-rate is one of the most influencing ones (see e.g., Kellner et al., 2019; Sinha, 1984; Timco and O.'Brien, 1994).

Dimension affected parameters can be transferred between scales with scaling laws. In ice model testing this is established by geometric scaling while maintaining the same Froude and Cauchy number in both scales (Schwarz, 1977; Timco and O.'Brien, 1994; von Bock und Polach and Molyneux, 2017). This means that the length, flexural strength and compressive strength are scaled with the geometric scaling factor λ and time scales with $\lambda^{0.5}$. This is the state of the art applied in model ice basins worldwide. However, shortcomings and drawbacks are also under discussion and scaling law inherited scale effects might depend on the actual loading scenario.

In order to reduce the possible effects of testing methods on the obtained results, International Towing Tank Conference (ITTC) gives recommendations on the testing procedures. ITTC (2014) gives two different length-width ratios for the uniaxial compressive strength specimen. However, as stated in the recommendations and noted by earlier studies (Li and Riska, 1996; von Bock und Polach and Ehlers, 2015), the ratio of specimen dimensions affect the determined nominal compressive strength.

Thus, this study aims to determine the effect of length-width ratio on the determined uniaxial compressive strength and sample behavior during the tests. In addition, the study focuses on the effect of the length-width ratio on the ratio between the uniaxial compressive and flexural strength and the strain modulus (i.e. the effective stiffness) determined from the compressive strength measurements. The applied data is gathered within extensive model ice property measurements conducted at the Hamburg Ship model Basin (HSVA) within European Union (EU) funded project Hydralab+. Furthermore, the relationship between the flexural and uniaxial compressive strength is determined in the beginning from full-scale measurements with a database (Kellner et al., 2019) analysis and later compared to the model-scale measurements. It should be noted that the uniaxial compressive strength is different than the compressive failure in the ice-structure interaction, due to the stress state. The uniaxial compressive strength is mainly a parameter of comparison as the flexural strength is.

The Relationship between Flexural and Compressive Strength in Full-Scale

The relationship between the flexural and compressive strength in full-scale is determined first in order to determine which values should be expected in model-scale. The basis for the analysis of the compressive strength in full-scale is the comprehensive database of Kellner et al. (2019). The database contains over 2000 entries of compressive strength tests for various grain structures, loading directions and water properties. In most cases, the model-scale ice is used to represent saline and columnar ice of type S2, which is the predominant ice type at sea. The gathered full-scale data needs to be aligned with the testing in model-scale.

In model-scale, the ice samples are compressively tested normal to the thickness direction. Furthermore, all tested model ice samples show a brittle failure and, therefore, the database is reduced to tests in which ice failed brittle, see Table 1. According to Kellner et al. (2019), the brittle failure occurs for temperatures below -9.95 ^{o}C and strain rates above $10^{-2.85}$ s^{-1}. The brittle failure also occurs at lower strain rates and temperatures below -16.35 ^{o}C (Kellner et al., 2019). Consequently, the database is reduced to samples with the following features: samples that are tested uniaxial and normal to the thickness direction, columnar grain structure, saline water and brittle failure. The obtained data points are shown in Figure 1.

Table 1. Database filter to compare brittle compressive failure with calculated flexural strength data

Temperature	Strain rate
-9.95 > T >-16.35	$>10^{-2.85}$
-16.35> T >-22.9	All strain rates

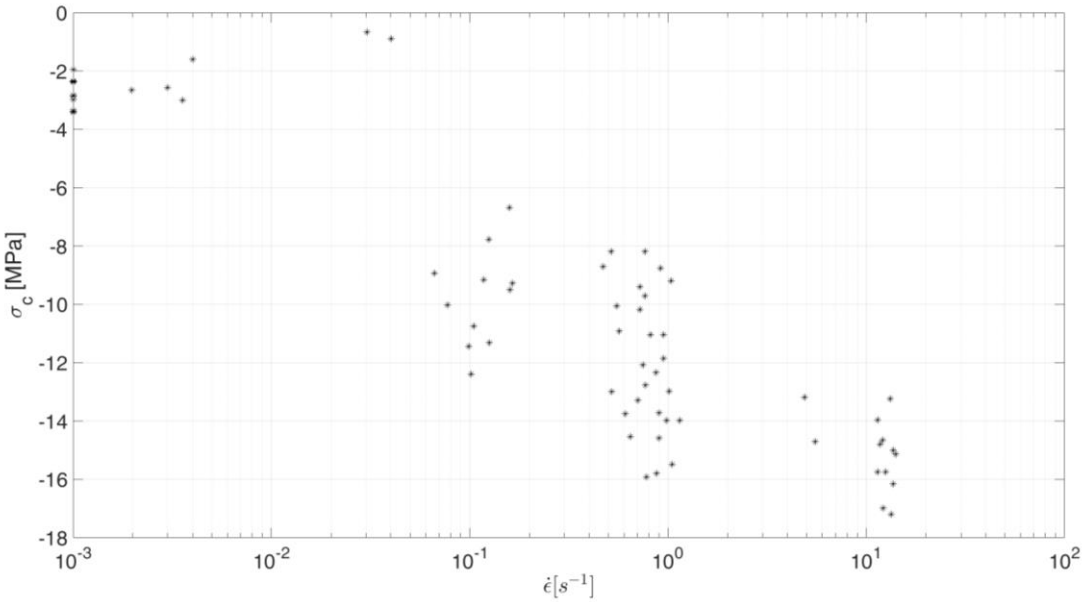

Figure 1. Brittle failing uniaxial compressive strength measurements in the horizontal direction as a function of a strain rate, $\dot{\varepsilon}$.

As the flexural strength is not simultaneously measured with the compressive strength, the flexural strength is determined through the regression formula determined by Timco and O.'Brien (1994). The flexural strength is calculated based on the brine volume, ν_b, which is determined from the temperature and salinity of ice as described by Frankenstein and Garner (1967).

As the validity of the regression formula refers to the temperature range -0.5 °C ≥ T_i ≥ -22.9 °C, the used data points from the compressive strength database is restricted to the same temperature range. The required input parameters to calculate the flexural strength are

extracted from the compressive strength database (Kellner et al., 2019). Despite many compressive strength tests have been conducted with saline sea water, only few feature actual salinity and temperature measurements. As the determination of the flexural strength requires information on the salinity and temperature, only the compressive strength measurements containing these features are extracted from the database. The flexural strength is calculated from the available data and is plotted on the particular strain-rate intervals that feature the selected compressive strength data (Figure 2). The mean value of the calculated flexural strength is 889 kPa.

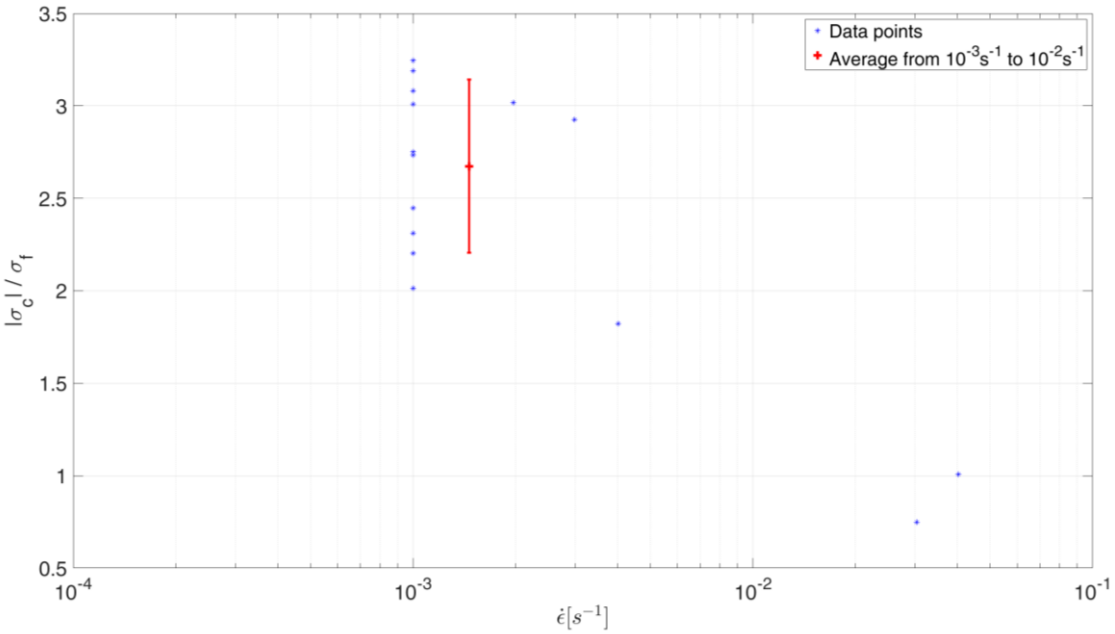

Figure 2. The ratio of the absolute value of the uniaxial horizontal compressive strength / flexural strength with an average value of 2.7 and a standard deviation of 0.47.

The average ratio of the horizontal compressive strength (absolute value) to the flexural strength for strain rates between 10^{-3} s^{-1} to 10^{-2} s^{-1} is 2.7 with a standard deviation of 0.47. At higher strain rates, the obtained ratio is significantly lower. However, due to a small number of data points, higher strain rates are not further evaluated. If the same procedure is repeated for compressive samples tested parallel to thickness with a strain rate of 10^{-3} s^{-1}, the ratio of the vertical compressive strength to flexural strength is in average 11.5 with a standard deviation of 8.48. Thus, the mean value for the compressive strength parallel to thickness is 4.3 times higher than for the compressive strength tested normal to the thickness.

TESTING METHODS AND SET-UP

This chapter briefly presents the test program, model ice, and methods and setup for the flexural and compressive strength tests. A more detailed presentation is given by Cáceres et al. (2018).

Test Program

The tests are conducted during a day in two cycles: with a higher bending strength in the morning and with a lower strength in the afternoon. The target ice thickness is 30 mm and the target bending strengths are 50 and 25 kPa. At the beginning of a measurement cycle, the strain modulus is measured according to the ITTC (2014) recommendations with the Hertz method, i.e. the deflection of an infinite plate. After the modulus is measured, the flexural strength measurements are conducted in-situ in five different locations along the basin. The samples for the uniaxial compressive strength test are cut and tested ex-situ simultaneously

with the flexural strength.

Model-scale Ice

HSVA's model ice is grown from a 0.7% sodium chloride solution in the natural way. The preparation of the ice sheet is started by a seeding procedure where the water is sprayed into the cold air of the ice tank. The droplets freeze in the air forming small ice crystals that settle on the water surface. Then the ice surface is exposed to cooled air. By this method the growth of a fine-grained ice of primarily columnar crystal structure is initiated. At the tank bottom is perforated water pipe with pressure-saturated water with air. This is uniformly discharged along the tank bottom during the entire freezing process. Immediately after discharging, the surplus air segregates from the water and forms tiny air bubbles. These air bubbles rise to the ice sheet, where they are embedded into the growing ice crystals. Due to the embedded air, the model ice fails more brittle and the density difference between ice and water is within the natural range (Evers and Jochman, 1993).

Flexural Strength

For the flexural strength tests, cantilever beams are cut to the ice sheet according to ITTC (2014) standards with the dimensions of 5-7 x h_{ice} in length and 2-3 x h_{ice} in breath (h_{ice}=ice thickness). In the test, a cantilever beam is pushed downward with a speed of 5 mm/s from the tip by a rod connected to a load cell. The applied load is measured throughout the test. The bending strength is defined as the tensile stress in the upper fiber due to downward bending, while assuming the ice as homogeneous and isotropic. It is calculated by the force maximum, length, breath and the ice thickness, as described in ITTC (2014).

Compressive Strength

The uniaxial compressive tests are conducted according to the ITTC (2014) standards in a cold room tempered at -1.4°C. As a difference to the guidelines, the dimensions (i.e. the aspect ratio) are varied in the tests. The breadth, w, of the samples is kept constant (2 x h_{ice}) while four different lengths, l, are applied (1, 2, 3, and 4 x h_{ice}). In the tests, a sample is placed vertically between two stainless steel plates, see Figure 3. While the upper plate is fixed and attached to a load cell, the bottom plate is vertically movable to generate the loading. The lower plate is adjusted in two modes: free to rotate and fixed. The lower plate is hydraulically driven upward with a velocity of 5 mm/s. The uniaxial compressive strength is determined as the maximum failure load divided by the horizontal cross-section. The (average) strain rate is defined as the deformation velocity / specimen height. Furthermore, the crack progression through the sample is documented in order to study the effect of the length-width ratio to the failure mechanism.

Figure 3. Ex-situ uniaxial compressive strength test.

ANALYSIS OF MEASUREMENTS IN MODEL-SCALE

The analysis focuses on the measurements with the lower flexural strength (measured to be 27.8 kPa in average) and the compressive strength measurements with the fixed bottom plate. The fixed bottom plate is chosen as it is a clearly defined boundary condition, while the rotatable bottom plate can lead to shear stresses due to confinement if tilted. The measured compressive strengths can be found from Cáceres et al. (2018). The raw data is given by Suominen and Haase (2018).

The Ratio between Compressive Strength and Flexural Strength

The compressive strength measurements show a significant scatter as the full-scale experiments, see Figure 4. The experiments show ratios of the compressive strength to the flexural strength between 1.1 and 2.7. However, the strength ratio appears to be smaller for the compressive strength samples having the length-width ratio (l/w) of 1.0, see Figure 4.

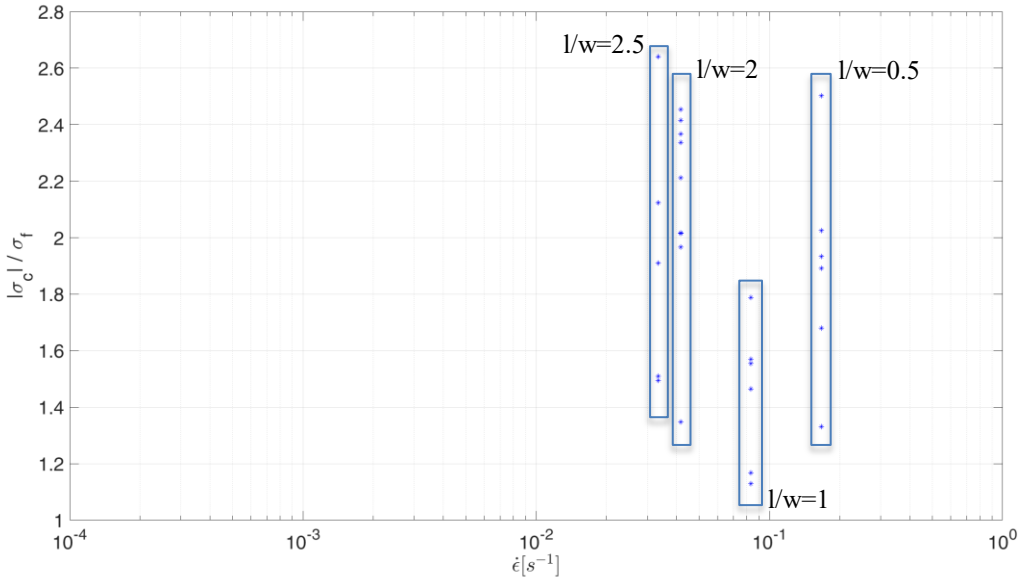

Figure 4. The ratio of the compressive strength and the flexural strength of model ice as a function of the strain rate for the experiments with a fixed bottom plate. The corresponding length/ width ratio, l/w, is stated for the particular results.

The model-scale data in Figure 4 occurs at a different strain rate regime than the full-scale data in Figure 2. Thus, the ratio of the compressive strength and the flexural strength cannot be compared directly between the scales on the basis of Figure 2 and Figure 4. Additionally, the strain rate contains a dimension which would need to be modified with respect to the scale. While acknowledging different view-points on the scaling approach, it is processed with the current state of the art following Froude and Cauchy similitude. For the strain rate, the relationship between model-scale, MS, and full-scale, FS, is given in Equation (1).

$$\dot{\varepsilon}_{FS} = \dot{\varepsilon}_{MS}\lambda^{-0.5} \tag{1}$$

In order to scale the mode-scale measurements in full-scale, a scaling factor has to be defined. Since the experiments in model-scale have not been designed to any scale of the experiments in the database (Kellner et al., 2019) directly, a dimension of reference needs to be selected. Here, the scaling factor is determined based on the flexural strength, which is scaled with the length scale λ directly (Zufelt and Ettema, 1996). The mean value of the calculated full-scale flexural strength measurements is 889 kPa, see INTRODUCTION. With the flexural strength in model-scale being 28 kPa, the scaling factor is consequently the ratio of 889 kPa / 28 kPa

resulting in λ = 31.57. The model-scale measurements are scaled to full-scale, by applying this scaling factor and are presented in Figure 5 with the full-scale measurements. For the analyzed measurements, the average ratio of uniaxial compressive strength to flexural strength in full-scale is 2.7 and in model-scale 2.06. As shown by Figure 5, the strength ratio of model-scale ice samples having the length-width ratio of 2 and 2.5 (i.e. $\dot{\varepsilon} < 10^{-2}\ s^{-1}$) is closer to the strength ratio of the full-scale ice samples.

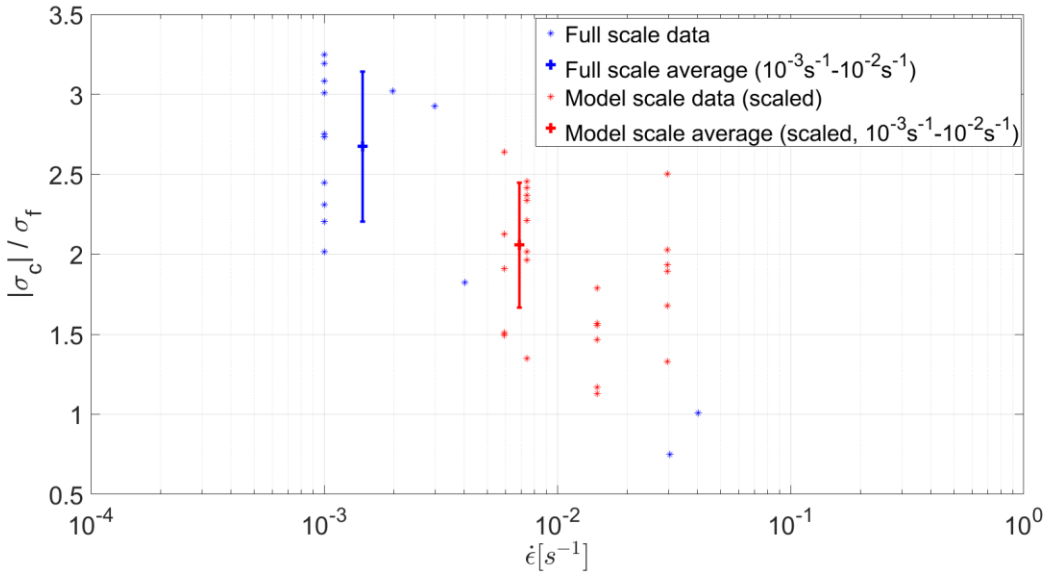

Figure 5. The compressive strength to flexural strength ratio for full-scale and model-scale data (scaled) as a function of the strain rate applied in the compressive strength tests.

Influence of Geometry on the Stiffness

The stiffness is represented with the strain modulus [MPa]. In the elastic domain, this strain modulus is identical to the elastic modulus or Young's modulus. However, as it is here unknown whether the regime is elastic or other, the term *strain modulus* is used. In order to determine the stiffness from the compressive strength measurements, the net strain and net stress between two points (e.g. 2 and 3 in Figure 6) is determined from which the stiffness in this particular section is determined. These two points must be connected by a steady load increase and not to be interfered by load relaxations due to cracking or splitting.

The question is, whether dependencies or correlations between the nominal compressive strength, and the specimen length-width ratio exist. Furthermore, the correlation between the nominal compressive strength, the displacement used for compactions (between 1 and 2, Figure 6), and the strain modulus exist. In order to evaluate these, the Pearson correlation (PCC) is used to assess whether a linear dependency between parameters exist. The PCC gives values between -1 and 1, where 1 represent a perfect positive linear correlation, -1 a perfect negative linear correlation and 0 no correlation at all. The cross-correlation matrix is shown in Table 2. The evaluation of the quality of linear correlation coefficients is done according to a suggestion of the Political Science Department at Quinnipiac University [1].

According to Table 2, a (very) strong dependency exists between the strain modulus and both the sample length-width ratio and the compressive strength. As the width and deformation speed are constant, the strain-modulus has also a very strong correlation with the strain rate, analogous to the length-width ratio. Also the pre-compression displacement seems to play a

[1] http://www.statisticshowto.com/probability-and-statistics/correlation-coefficient-formula/, 13.09.2018

role, where the specimen is presumably compacted before a linear load increase is shown.

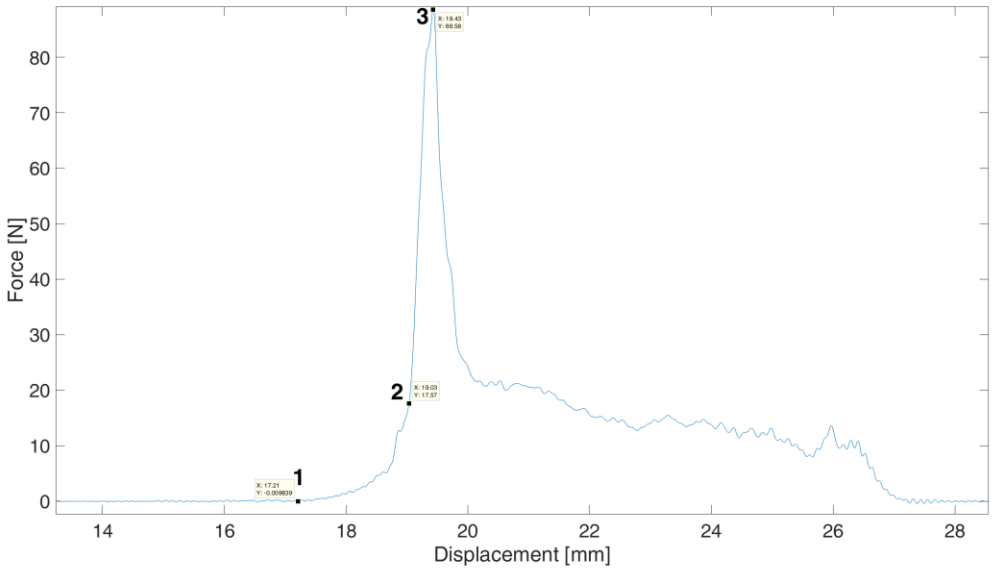

Figure 6. A compressive strength measurement with evaluation points: 1) Start of a load application with compaction and load increase until 2), this phase is termed: pre-compression. 2) Start of a steady load increase until a failure at 3), over which the stiffness is determined.

Table 2. PCC coefficients between parameters.

	Strain Modulus	Compressive strength	Specimen length-width ratio	Pre-compression displacement
Strain modulus	1	0.63	0.69	-0.33
Compressive strength	0.63 (strong)	1	0.26	00.49
Specimen length-width ratio	0.69 (strong – very strong)	0.26 (weak)	1	-0.40
Pre-compression displacement	-0.33 (moderate)	-0.49 (strong)	-0.40 (strong)	1

Failure Patterns

The observed failure patterns are displayed in Figure 7 and are divided into six categories: 1) Y-shape, 2) V-shape (not starting from/ending to the corners of the sample), 3) I-shape (sample splits in longitudinal direction), 4) V-shape starting/ending from/to a corner of the sample, 5) X-shape, 6) Combination of failure mechanism.

The failure pattern depends significantly on the sample dimensions. Patterns 1-3 are observed only for samples having a length-width ratio over 2.0, while patterns 4-5 were observed with samples having a length-width ratio of 1.0. The failure patterns of the samples having a length equal to the thickness (failure pattern #6) cannot be defined uniquely from recorded videos or by visual observations. These samples seem to fail simultaneously from several locations with V and I-shaped failure patterns.

Figure 8 presents the measured compressive strength values and strain modules for the different observe failure modes. In one case, the sample failed from the left-hand-side corner

simultaneously to a through length split. As both failure modes are considered significant, the failure mode is marked as 2.5, a combination of mode 2 and 3, in Figure 8. In another case, the sample failed from both sides as V shaped and from the middle as Y-shape. Following the same naming principle, the failure mode is named 1.5 in Figure 8. Other samples are classified in one of afore mentioned failure pattern groups.

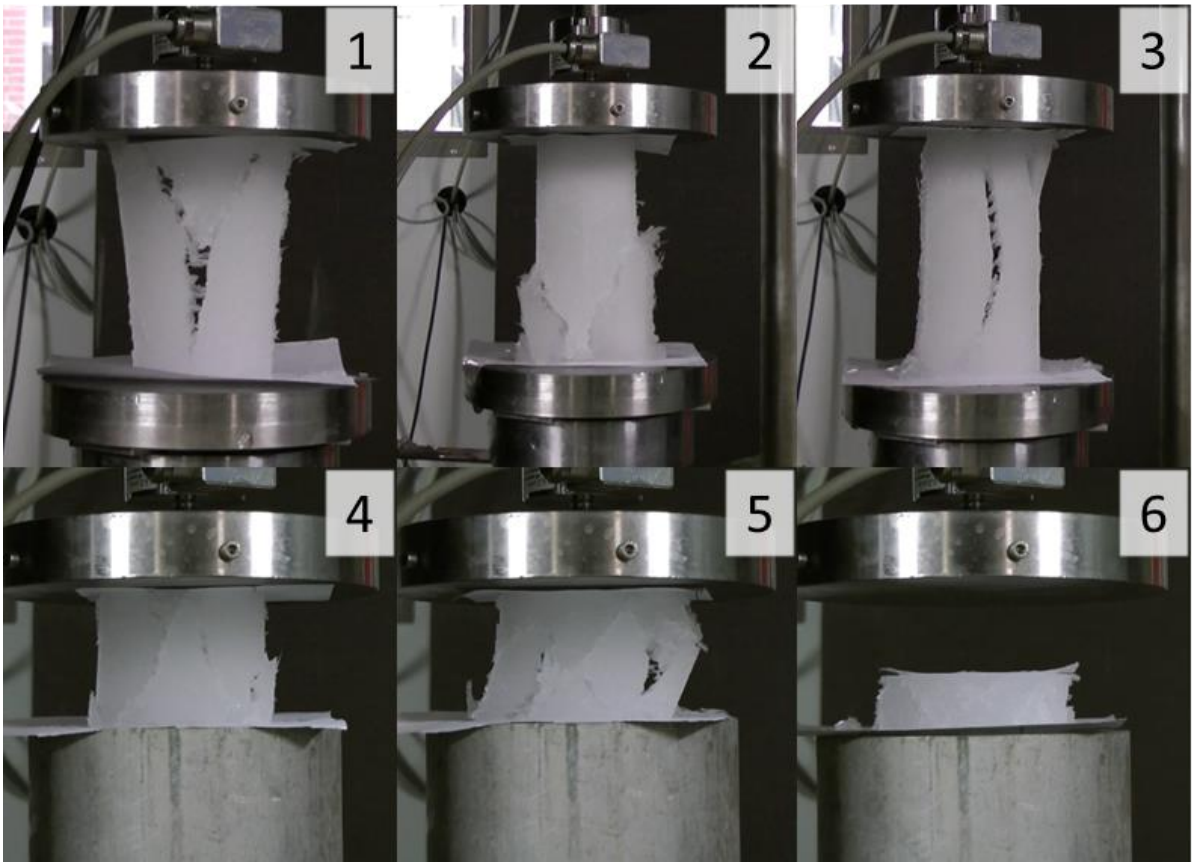

Figure 7. Different failure patterns observed in the compressive strength tests.

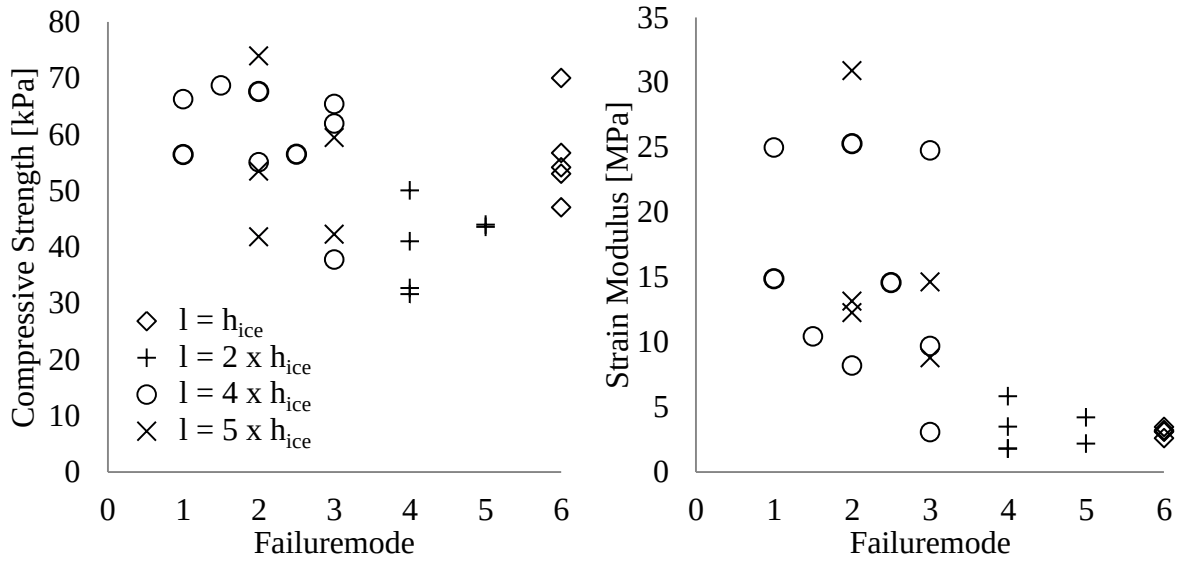

Figure 8. The measured compressive strength and strain modulus for different failure modes.

Figure 8 shows no clear difference between the failure modes 1-3 for the compressive strength or strain modulus, despite a great scatter in the measurements. However, the trend shows that the compressive strength measured with samples having a length-width ratio of

1.0 (failure modes 4 and 5) is generally lower than with samples having a larger ratio (failure modes 1-3). Furthermore, the strain modulus for the square samples is significantly smaller than for the longer samples. The failure modes in class 6, i.e. samples with the smallest ratio, are combinations of all failure modes.

DISCUSSION

In section 5 of the ITTC guideline 7.5-02-04-02, it is stated that the deformation speed should be sufficiently high to cause a brittle failure. However, different recommendations for test geometries are given. This is due to the fact that various ice tanks have been developing their own methods. The investigation in this paper, as well as in von Bock und Polach and Ehlers (2015) and Li and Riska (1998), indicates an impact of the geometry on the obtained nominal uniaxial compressive strength. Until now it is not established which test geometry might be more suitable to reflect full-scale experiments well. It is important to state that the goal is not to achieve a nominal compressive strength in model-scale that scales well, but to define a geometry that reflects the failure mechanisms in full-scale adequately. Therefore, this study serves to provide a better understanding of processes involved in model-scale ice. Despite all samples in the presented study fail brittle, a strain rate effect is evident, but the aspect of strain rate is not accounted yet in the model testing guidelines. Within the regime of brittle failure, the strain rate has an impact on the nominal compressive strength as found in full-scale. However, it is unclear to what extend this applies on model ice and if this can be accounted by simply adjusting the length of the test specimen.

As discussed by Li and Riska (1996), the failure should not happen through the corners of the sample, as in these cases, the stress concentration in the corners affect the results. This type of failure pattern occurred in samples having a length-width ratio of 1.0 in three of five tests, but for no sample having a length of four times the thickness. The study of Li and Riska (1996) showed that the minimum length for the compressive strength of ice tests with fine-grained ethanol ice is 2.7 times the thickness. Thus, these tests suggest that the ITTC recommendation for the length of the sample of four times the thickness would be preferable for the fine-grained ethanol and saline columnar model-scale ice if the assessment is solely based on the nominal compressive strength and based on reducing the possible effect of stress concentration on corners. It needs to be acknowledged that Li and Riska (1996) as well as von Bock und Polach and Ehlers (2013) investigated in-situ experiments, where one end of the attached specimen was still attached to the parent ice sheet and I-cracks (crack mode 3 in Figure 7) have not been observed. The latter might have an impact on the failure development and therewith also on the compressive strength, but it remains unknown to what extent.

As the model scale measurements are conducted without any particular scale, the scaling factor is defined based on the ratio between the flexural strength in model-scale and full-scale measurements. Commonly, the uniaxial compressive strength in full-scale measurements is measured with samples that are portions from the through thickness height of ice, whereas the flexural strength is measured with beams of the entire ice thickness, i.e. through thickness samples. In model scale, both of the strengths are measured with through thickness samples, i.e. the size of the samples is in a similar range. For this reason, the geometric scaling factors determined from the size of the tested samples, would result in different scaling factors. As the time is also scaled based on the Froude scaling law, the time-scaled time and consequently the scaled strain rate (Figure 9) is significantly affected the used scaling factor. Thus, it should be kept in mind that the determination of the scaling factor in this regard is not straight forward and will affect the presented results. Furthermore, the scaling itself is not trivial and the validity of the Froude scaling law for the strength measurements has been subjected to discussion for decades (Atkins and Caddell, 1974; Palmer and Dempsey, 2009; Schwarz, 1977; von Bock und Polach and Ehlers, 2015; von Bock und Polach and Molyneux,

2017). With respect to difficulties as described in this paper von Bock und Polach and Molyneux (2017) suggested case based scaling, i.e. not applying a global scaling approach on ice model tests, but different ones that account for particular effects and governing loads of the interaction scenario.

Von Bock und Polach and Ehlers (2013) have indicated that the elastic modulus or strain modulus determined by the Hertz-method may not reflect the stiffness encountered in compression. However, the strain modulus measured in accordance to ITTC (2014) recommendations from the investigated ice sheet is around 3 MPa (Cáceres et al., 2018) and the results reported here show that the strain modulus is at this range with the specimen having a length-width ratio of 1 and 0.5. Thus, further investigation on this matter is needed.

CONCLUSIONS

The ITTC guidelines give recommendations for two different length-width ratios for the samples to be used for the determination of the compressive strength, 1.0 and 2.0. However, the results show that the length-width ratio of the compressive strength sample affects the measured compressive strength, failure pattern, and the strain modulus determined from the compressive strength measurements. Additionally, there are indications that different failure developments in-situ and ex-situ occur and it needs to be investigated to what extend those affect the compressive strength.

ACKNOWLEDGEMENTS

The work described in this publication was supported by the European Community's Horizon 2020 Research and Innovation Programme through the grant to HYDRALA-PLUS, Contract no. 654110. The authors would like to thank HSVA's Ice Tank personnel (Dalley Mario, Gehrisch Steve, Koch Roland, Krywald Roman, Schnoor Nis, Toure Mohamed, von Frieling Björn) and an internship student Aaron Tam for their work and help during the tests.

References

Atkins, A.G. & Caddell, R.M., 1974. The laws of similitude and crack propagation, *International Journal of Mechanical Sciences*, vol. 16, no. 8, pp. 541–548.

Cáceres, I., Suominen, M., Haase, A., Grasso, F., Houseago, R., van der Aad, O., O'Donoghue, T., McLelland, S., Parsons, D., Hurter, D., Thorne, P., Sánchez-Arcilla, A., Cooke, R., Sospedra, J., Estre Musumeci, R., Iuppa, C., Staudt, F., Schimmels, S., Dupuis, V., Moulin, F. & Williams, H., 2018. *Deliverable 9.5: Collection of Benchmark data sets. Work package 9 – Cross disciplinary Observations of Morphodynamics and Protective structures Linked to Ecology and eXtreme events:* Hydralab+ project.

Evers, K.-U. & Jochman, P., 1993. An Advanced Technique to Improve the Mechanical Properties of Model Ice Developed at the HSV A Ice Tank, *International Conference on Port and Ocean Engineering under Arctic Conditions (POAC) 93.*

Frankenstein, G. & Garner, R., 1967. Equations for Determining the Brine Volume of Sea Ice from −0.5° to −22.9°C, *Journal of Glaciology*, vol. 6, no. 48, pp. 943–944.

ITTC, 2014. *Ice property measurements, 7.5-02-04-02* [Online], International Towing Tank Conference, 7.5-02-04-02.

Jordaan, I. J., 2001. Mechanics of ice–structure interaction, *Engineering Fracture Mechanics*, vol. 68, 17-18, pp. 1923–1960.

Kellner, L., Stender, M., von Bock und Polach, Rüdiger U. Franz, Herrnring, H., Ehlers, S.,

Hoffmann, N. & Høyland, K. V., 2019. Establishing a common database of ice experiments and using machine learning to understand and predict ice behavior, *Cold Regions Science and Technology*, vol. 162, pp. 56-73.

Lau, M., Wang, J. & Lee, C., 2007. Review of Ice Modelling Methodology, *International Conference on Port and Ocean Engineering under Arctic Conditions (POAC) 2007.*

Li, Z. & Riska, K., 1996. *Preliminary study of physical and mechanical properties of model ice*, Otaniemi, Helsinki University of Technology, Ship Laboratory.

Li, Z. & Riska, K., 1998. Uniaxial compressive strength of fine grain ethanol model ice, *Ice in Surface Waters.* Rotterdam, Balkema.

Muggeridge, D. B., ed., 1977. *POAC 77, St. John's*, Memorial University of Newfoundland.

Palmer, A. and Dempsey, J., 2009. Model Tests in Ice, *International Conference on Port and Ocean Engineering under Arctic Conditions (POAC) 09*.

Schwarz, J., 1977. New Developments in Modeling Ice Problems, *International Conference on Port and Ocean Engineering under Arctic Conditions (POAC) 77*.

Sinha, N. K., 1984. Uniaxial compressive strength of first-year and multi-year sea ice, *Canadian Journal of Civil Engineering*, vol. 11, no. 1, pp. 82–91.

Suominen, M. & Haase, A., 2018. *Compressive Strength Of Model Ice Measurements*. DOI:10.5281/zenodo.1441110

Timco, G. W. & O.'Brien, S., 1994. Flexural strength equation for sea ice, *Cold Regions Science and Technology*, vol. 22, no. 3, pp. 285–298.

von Bock und Polach, R. U. F. & Ehlers, S., 2013. Model scale ice — Part B: Numerical model, *Cold Regions Science and Technology*, vol. 94, pp. 53–60.

von Bock und Polach, R. U. F. & Ehlers, S., 2015. On the Scalability of Model-Scale Ice Experiments, *Journal of Offshore Mechanics and Arctic Engineering*, vol. 137, no. 5, p. 51502.

von Bock und Polach, R. U. F. & Molyneux, D., 2017. Model Ice: A Review of its Capacity and Identification of Knowledge Gaps, *Proceedings of the ASME 36th International Conference on Ocean, Offshore and Arctic Engineering 2017*.

Zufelt, J. & Ettema, R., 1996. *Model Ice Properties,* U.S. Army Corps of Engineers, Cold Regions Research and Engineering Laboratory (CRREL) CRREL Report 96-1.